Enhancement of HERG K^+ Currents by Cd^{2+} Destabilization of the Inactivated State

J. P. Johnson, Jr.,* Jeffrey R. Balser,*# and Paul B. Bennett*
Departments of *Pharmacology and #Anesthesiology, Vanderbilt University School of Medicine, Nashville, Tennessee 37232-6602 USA

ABSTRACT We have studied the functional effects of extracellular Cd^{2+} on human *ether-à-go-go*-related gene (HERG) encoded K^+ channels. Low concentrations (10–200 μM) of extracellular Cd^{2+} increased outward currents through HERG channels; 200 μM Cd^{2+} more than doubled HERG currents and altered current kinetics. Cd^{2+} concentrations up to 200 μM did not change the voltage dependence of channel activation, but shifted the voltage dependence of inactivation to more depolarized membrane potentials. Cd^{2+} concentrations $\geq$500 μM shifted the voltage dependence of channel activation to more positive potentials. These results are consistent with a somewhat specific ability of Cd^{2+} to destabilize the inactivated state. We tested the hypothesis that channel inactivation is essential for Cd^{2+}-induced increases in HERG K^+ currents, using a double point mutation (G628C/S631C) that diminishes HERG inactivation (Smith, P. L., T. Baukrowitz, and G. Yellen. 1996. *Nature (Lond.).* 379:833–836). This inactivation-removed mutant is insensitive to low concentrations of Cd^{2+}. Thus, Cd^{2+} had two distinct effects on HERG K^+ channels. Low concentrations of Cd^{2+} caused relatively selective effects on inactivation, resulting in a reduction of the apparent rectification of the channel and thereby increasing HERG K^+ currents. Higher Cd^{2+} concentrations affected activation gating as well, possibly by a surface charge screening mechanism or by association with a lower affinity site.

INTRODUCTION

The human *ether-à-go-go*-related gene K^+ channel (HERG) is a member of the EAG family of voltage-gated K^+ channels (Warmke and Ganetzky, 1994) and has been identified as the molecular basis for the rapid delayed rectifier K^+ current in human heart (I_{Kr}) (Sanguinetti et al., 1995). Mutations in HERG cause one form of the congenital long QT syndrome (LQT2) (Sanguinetti et al., 1995, 1996), and pharmacologic block of HERG K^+ channels in heart can result in QT prolongation and arrhythmias (acquired LQT) (Roy et al., 1996; Choy et al., 1997; Rampe et al., 1997). HERG K^+ channels display rapid inactivation gating, which causes an apparent inward rectification of the current-voltage relationship (Trudeau et al., 1995; Sanguinetti et al., 1995; Smith et al., 1996; Spector et al., 1996; Schönherr and Heinemann, 1996). The unusual kinetics of HERG gating make separation and description of specific gating properties difficult. We recently found that extracellular Ca^{2+} can modulate the voltage dependence of HERG channel activation independently of inactivation (Johnson et al., 1999). The ability to separately modify the voltage dependence of activation with Ca^{2+} adds to the mounting evidence that, unlike *Shaker* K^+ channels, HERG inactivation gating has intrinsic voltage dependence distinct from that of activation (Wang et al., 1996; Zou et al., 1998). It was previously shown that another inorganic divalent cation, Cd^{2+}, modulates cat ventricular I_K and rabbit ventricular I_{Kr} (Follmer et al., 1992; Paquette et al., 1998). In both cases the voltage-dependent activation of the currents is shifted to more depolarized potentials, while the maximal current level was paradoxically increased. We therefore studied the response of cloned HERG channels to extracellular Cd^{2+} in order to determine whether these channels can be modulated by Cd^{2+}, and if so, to determine the biophysical nature of the interaction. The present study illustrates that low concentrations of extracellular Cd^{2+} modulated voltage-dependent HERG inactivation independently of channel activation. Thus, there appear to be at least two distinct divalent cation interaction sites on the extracellular face of HERG channels; one that modulates activation, and another that modulates inactivation.

MATERIALS AND METHODS

Plasmid cDNA constructs

The HERG cDNA, obtained from Dr. Mark Keating (University of Utah), was ligated into the pSI mammalian expression plasmid (Promega, Madison, WI). The CD8 antigen gene in the EBO-pcD Leu-2 vector was kindly provided by Dr. Richard Horn (Jefferson Medical College). CD8 is a human T lymphocyte surface antigen and was used to visually identify transfected cells using CD8 antibody-coated polystyrene microbeads. The HERG G628C/S631C mutant cDNA was a gift of Dr. Gary Yellen (Harvard University).

Cells

Chinese hamster ovary K1 (CHO-K1) cells were obtained from the American Type Culture Collection (Rockville, MD) and maintained in HAMS F-12 media (GibcoBRL, Grand Island, NY) supplemented with 1 mM L-glutamine and 10% heat inactivated fetal bovine serum (GibcoBRL) in a humidified, 5% CO_2 incubator at 37°C.

Received for publication 26 February 1999 and in final form 8 June 1999.
Address reprint requests to Dr. Paul B. Bennett, Senior Director, Ion Channel Research Pharmacology WP26-265, Merck Research Laboratories, 770 Sumneytown Pike, West Point, PA 19486. Tel.: 215-652-4013; Fax: 215-652-0800; E-mail: paul bennett@merck.com.

0006-3495/99/11/2534/08 $2.00

Transfection

CHO-K1 cells were co-transfected with the HERG and CD8 plasmids in a ratio of 4:1. Transfection was accomplished using the Lipofectamine transfection reagents and method (GibcoBRL). Immediately before patch clamping, cells were labeled with commercially prepared microbeads conjugated to CD8 antibodies (DynaBeads from Dynal, Oslo, Norway) to identify transfected cells. Cells that displayed CD8 on their surface bound DynaBeads, indicating successful transfection (Jurman et al., 1994).

Solutions

The intracellular recording solution for all experiments was (in mM): 110 KCl, 5 K_2ATP, 5 K_4BAPTA, 2 $MgCl_2$, 10 HEPES, pH 7.2. The control extracellular recording solution was (in mM): 145 NaCl, 4 KCl, 1.8 $CaCl_2$, 1 $MgCl_2$, 10 HEPES, 10 glucose, pH 7.35. Cd^{2+} solutions were made by adding an appropriate amount of 1 M aqueous $CdCl_2$ solution to the control extracellular solution.

Electrophysiology

HERG channel function was studied with the whole-cell patch clamp technique (Hamill et al., 1981). Cells were studied 36–60 h after transfection, and all experiments were done at room temperature (23–25°C). Recordings were made using an Axopatch 200A patch clamp amplifier in conjunction with a Digidata 1200 interface (Axon Instruments, Foster City, CA). Patch pipettes were fabricated from Radnotti (Monrovia, CA) 1.2-mm outside diameter starbore capillary glass using a Flaming/Brown micropipette puller (model P-97, Sutter Instruments Co., Novato, CA). Patch pipette resistances were 1–2 MΩ. Cell and pipette capacitances were nulled and series resistance was compensated ≥85% before recording. Data were acquired using pCLAMP programs (version 6.03, Axon Instruments). All raw current recordings are shown with the bottom of the current scale bar indicating zero current.

Data analysis

Data were analyzed and plotted using a combination of pCLAMP, Origin (Microcal Software, Northampton, MA), and SigmaPlot (Jandel Scientific, San Rafael, CA) software. Half-maximal voltages ($V_{1/2}$) and slope factors (k_v) of activation and inactivation were determined by fitting the data with a Boltzmann function of the form $I_{max}/(1 + \exp([V - V_{1/2}]/k_v)$, where I_{max} is the limiting amplitude. Time constants (τ) of inactivation and deactivation were determined by fitting the data with a single exponential equation: $A \cdot \exp(-t/\tau) + C$, where A is an amplitude term, t is time, and C is a constant.

RESULTS

Fig. 1 shows two families of HERG K^+ currents from the same transiently transfected CHO-K1 cell, one in control solutions and another in 200 μM external Cd^{2+}. Depolarizing voltage clamp steps result in currents that appear to inwardly rectify due to voltage-dependent fast inactivation (Smith et al., 1996; Spector et al., 1996; Schönherr and Heinemann, 1996). Repolarization to −50 mV results in the large tail currents that are characteristic of HERG. These tail currents are the result of rapid recovery of channels inactivated by the preceding test pulse (rising phase) followed by a slow return of channels to the rested closed state (falling phase). Surprisingly, 200 μM Cd^{2+} enhanced HERG outward currents at most tested membrane potentials. This

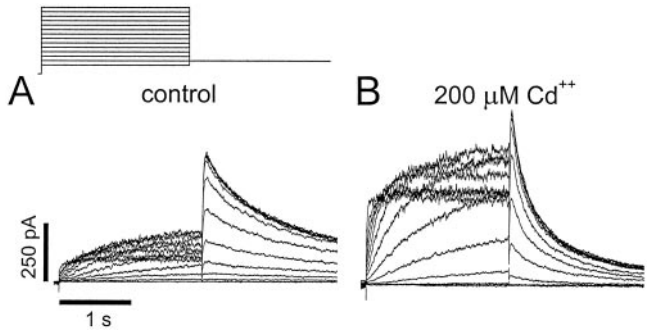

FIGURE 1 Cd^{2+} enhances HERG K^+ currents. HERG currents recorded from the same cell in the absence (*A*) or presence (*B*) of 200 μM Cd^{2+}. The voltage clamp protocol is shown at the top left. The membrane potential was held at −80 mV. A test step to potentials between +70 and −70 mV was then followed by repolarization to −50 mV.

concentration of Cd^{2+} also significantly decreased the time constant of current decay at −50 mV from 1.23 ± 0.27 s to 0.47 ± 0.11 s (paired *t*-test $p < 0.05$, $n = 4$). As mentioned above, the rate of tail current decay is reflective of the rate of channel closure related to the activation/deactivation process, but the complexity of HERG gating introduces the need for caution in interpreting the meaning of observed current time dependences. Because we observed an increase in the rate of decay of the tail currents, we examined the time course of current onset to determine whether Cd^{2+} was affecting the activation process.

Fig. 2 *B* shows the time dependence of HERG current development at +20 mV in control solutions and in 200 μM Cd^{2+} measured by an envelope of tail currents. This envelope of tails test provides the best method for separating the time course of current activation from inactivation (Wang et al., 1997a). In contrast to the altered rate of tail current decay, the time course of channel activation at +20 mV was unchanged by 200 μM Cd^{2+}. These data suggest several possibilities: 1) Cd^{2+} blocks the channel in a time-dependent fashion at negative but not at positive membrane potentials (this could explain the acceleration of the tail current decay, but would not account for increased outward currents); 2) activation and deactivation are distinct processes affected differentially by Cd^{2+}; or 3) Cd^{2+} does not really affect the activation/deactivation process at all, but alters the tail current decay by some indirect mechanism.

In order to understand how extracellular Cd^{2+} enhanced HERG currents we examined the voltage dependence of channel activation in different concentrations of external Cd^{2+} using the voltage clamp protocol in Fig. 1. Figs. 3 and 4 show the results of paired experiments where measurements in each Cd^{2+} concentration were normalized to the control peak tail current value in the same cell (see legends to Figs. 3 and 4). In Fig. 3 data are presented that demonstrate that 10 μM extracellular Cd^{2+} significantly enhanced HERG currents during positive test potentials (paired Student's *t*-test values <0.05 for voltages between −20 mV and +60 mV). Increasing the Cd^{2+} concentration to 100 or

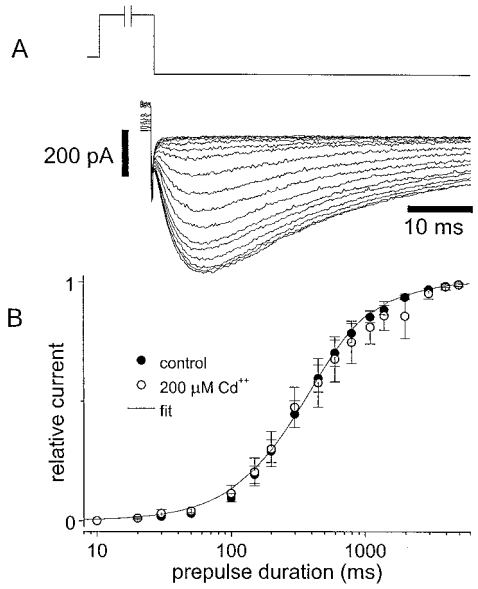

FIGURE 2 The rate of HERG activation is not affected by 200 μM Cd^{2+}. An envelope of tails protocol illustrated at the top of (*A*) was used to determine the rate of activation. Cells were held at −80 mV before a step of variable duration to +20 mV. The membrane potential was then stepped to −120 mV and the peak inward current was measured. A typical recording in control conditions is shown at the bottom of (*A*). Peak current measurements were normalized by dividing all currents by the current after a 5-s prepulse and then averaged. These averaged current values were then plotted against the duration of the prepulse to +20 mV (*B*). The values in (*B*) are averages of paired measurements from four cells. Error bars represent standard error of the mean. The smooth curve in (*B*) is a two-exponential fit [$y = A_1 \cdot \exp(-t/\tau_1) + A_2 \cdot \exp(-t/\tau_2) + C$] to the control data.

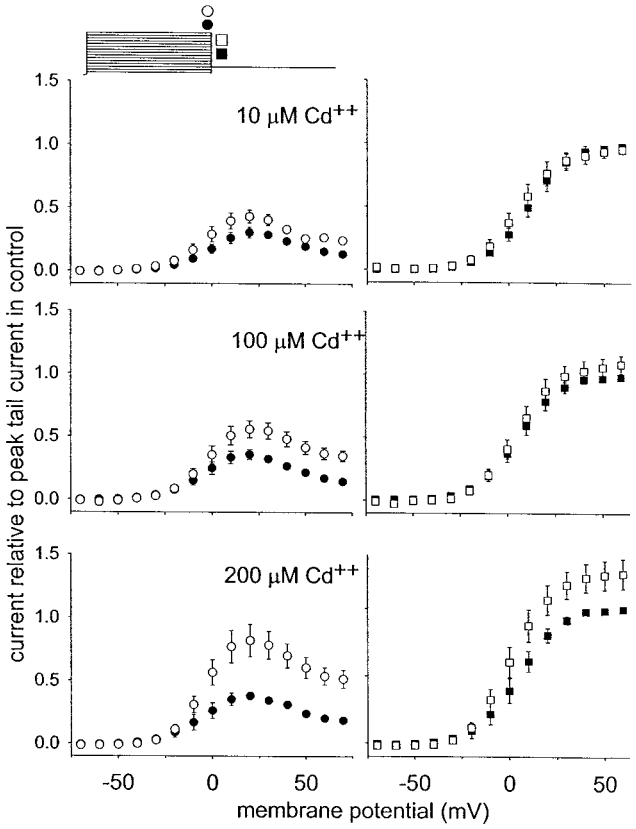

FIGURE 3 Voltage dependence of activation in low extracellular Cd^{2+}. Current-voltage relationships were generated with the voltage clamp protocol in Fig. 1. The protocol is shown at the top left of this figure, and the symbols above it indicate the times at which the current was measured for the curves below. Circles (*left side*) indicate the current measurement was made at the end of the step to the test potential. Squares (*right side*) indicate the peak tail current after repolarization to −50 mV. Filled symbols indicate control extracellular solution. Open symbols indicate Cd^{2+} solution. The Cd^{2+} concentrations labeled on the left apply also the tail current measurements on the right. In each case the average values shown come from paired measurements in several cells ($n = 3$ in 10 μM; $n = 5$ in 100 μM; $n = 6$ in 200 μM). Current in each cell was normalized to the maximal tail current in control conditions before averaging. Error bars indicate standard error of the mean and are shown for each point.

200 μM caused even greater increases in HERG current. In 200 μM Cd^{2+} HERG K^+ current at +20 mV was increased by 2.2 ± 0.3-fold compared to control ($p < 0.05$, $n = 6$), and currents at +70 mV were increased 2.8 ± 0.4-fold ($p < 0.005$). Peak tail current amplitudes upon repolarization to −50 mV were also increased (1.29 ± 0.11-fold, $p < 0.05$). External Cd^{2+} ≤200 μM did not change either the slope factor (k_V) or the half-maximal voltage ($V_{1/2}$) of HERG activation as determined from the tail current voltage relationship (Fig. 3, *right side*). The slope factors of the tail current-voltage relationship were 9.4 ± 0.4 mV in control solution and 8.8 ± 0.5 mV in 200 μM Cd^{2+}. The $V_{1/2}$ was −4.9 ± 2.9 mV in control solution and −3.6 ± 3.8 mV in 200 μM Cd^{2+} (see Fig. 5).

Fig. 4 shows a summary of data in which higher concentrations of external Cd^{2+} were applied to HERG-expressing cells. Increasing the Cd^{2+} concentration from 0.5 to 10 mM produced concentration-dependent rightward shifts in the $V_{1/2}$ of activation (Fig. 4). This increase in the potential required to open the channels resulted in decreased HERG currents at some potentials. However, at very positive voltages, where the open probability of the Cd^{2+}-treated cells is higher, currents in the presence of Cd^{2+} remain larger than the same cell control currents. Thus, Cd^{2+} had two distinct effects on HERG currents. At low concentrations (10–200 μM), Cd^{2+} enhanced HERG currents without shifting the voltage dependence of activation. Higher concentrations of Cd^{2+} (0.5–10 mM) shifted the voltage dependence of channel activation to more depolarized potentials.

Fig. 5 illustrates the Cd^{2+} concentration dependence of the shift of HERG voltage dependence of activation. The difference between the half-maximal voltage of current activation in control and Cd^{2+} solutions was determined by paired tail current measurements in the same cells (see legend). Cd^{2+} concentrations of from 10 to 200 μM had no significant impact on the $V_{1/2}$ of activation ($p < 0.05$). However, raising Cd^{2+} to 0.5 mM shifts the $V_{1/2}$ of activation +14.4 ± 3.1 mV ($p < 0.05$), and further increases of the Cd^{2+} concentration lead to still larger shifts in the voltage dependence of activation. This indicates that 200 μM approaches a threshold concentration beyond which Cd^{2+} affected HERG activation gating.

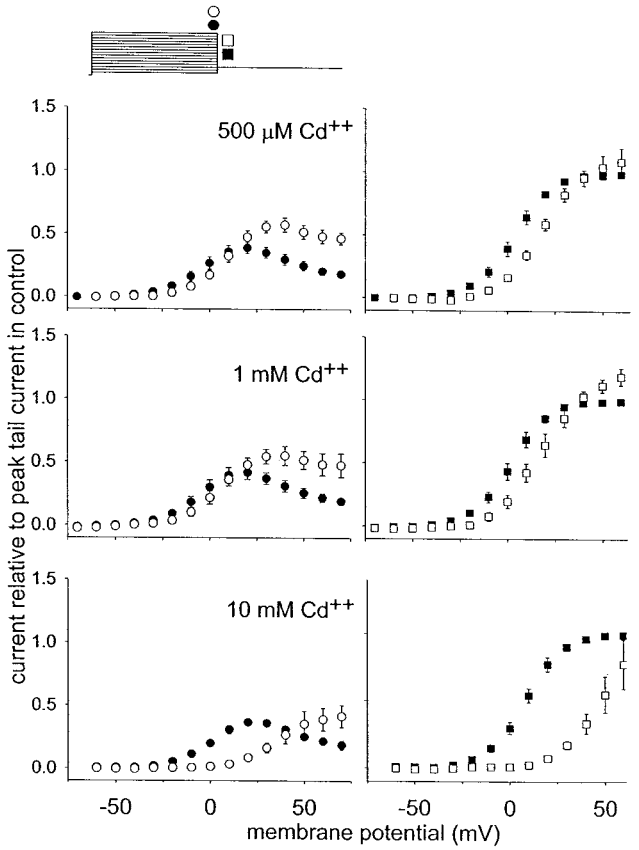

FIGURE 4 Voltage dependence of activation in high extracellular Cd^{2+}. Current-voltage relationships created as in Fig. 3 (see legend), except with higher concentrations of extracellular Cd^{2+} ($n = 4$ in 0.5 mM; $n = 4$ in 1 mM; $n = 2$ in 10 mM).

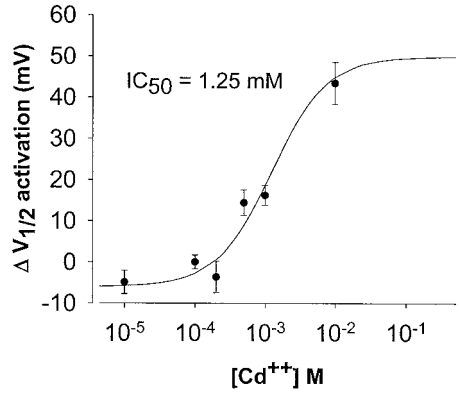

FIGURE 5 The data used to generate the peak tail current-voltage relationships on the right of Figs. 3 and 4 were used to determine the change in the $V_{1/2}$ of activation in different concentrations of Cd^{2+}. A Boltzmann equation (see Methods) was fit to the peak tail current-voltage relationship in control and Cd^{2+}-containing solutions. The $V_{1/2}$ determined in this manner for control solution was then subtracted from the $V_{1/2}$ measured in Cd^{2+} solution ($V_{1/2}$ in Cd^{2+} − $V_{1/2}$ in control). The difference between the $V_{1/2}$ values was plotted versus the Cd^{2+} concentration. The smooth curve was generated using a logistic equation with an IC_{50} of 1.25 mM. Error bars indicate the standard error of the mean.

The shift in the voltage dependence of activation caused by high concentrations of Cd^{2+} could be due to nonspecific screening of membrane surface charges or to Cd^{2+} binding to the channel at a relatively low-affinity site. Enhancement of HERG currents by low Cd^{2+} concentrations cannot be explained by nonspecific changes in the membrane electrical field through charge screening, since this would cause the voltage dependence of activation to be shifted to more depolarized potentials and thus would reduce, not increase, K^+ currents. Figs. 3 and 5 show that 200 μM Cd^{2+} is the highest tested Cd^{2+} concentration that did not shift the voltage dependence of channel activation; therefore, we further explored the mechanism of Cd^{2+} potentiation at this concentration. A simple mechanism by which Cd^{2+} could increase HERG currents is to decrease the probability that the channels inactivate. To test whether Cd^{2+} changed the rate of HERG inactivation, we used a three-step voltage-clamp protocol (Smith et al., 1996; Spector et al., 1996; Wang et al., 1996). Channels were activated and inactivated by a prepulse to +70 mV, allowed to rapidly recover at −100 mV, and then the rate of channel inactivation was observed during the third step to the test potential. A mono-exponential fit of the inactivating K^+ currents was used to estimate a time constant for inactivation (see Methods). The time constants derived from paired experiments in zero and 200 μM Cd^{2+} are plotted versus the test potential in Fig. 6 *B* and show that Cd^{2+} significantly increased the time constants of channel inactivation in the same range of membrane potentials where the currents are increased (Fig. 3).

Fig. 7 *B* shows the effect of 200 mM Cd^{2+} on the voltage dependence of channel open-inactivated distribution ("inactivation availability"). Another three-pulse voltage clamp protocol was used to make these measurements (see legend) (Smith et al., 1996; Spector et al., 1996). The dynamic nature of HERG currents precludes direct measurements of "steady state" inactivation, but the data shown approximate a voltage dependence of the distribution of channels between open and inactivated states. A 3-s step to +70 mV fully activates and inactivates the channels. The second step to the test potential then allows some fraction of the channels to recover from inactivation. The instantaneous current after the third step to +30 mV allows measurement of the fraction of channels that have recovered from inactivation during the preceding test step. Currents were normalized to the maximum current value for each cell to allow averaging between cells (paired measurements, nine cells). Cd^{2+} (200 mM) shifted the voltage dependence of channel availability (determined by a Boltzmann fit) by +21 ± 5 mV. The half-maximal voltage of availability ($V_{1/2}$) was −90.6 ± 2.6 mV in control solution and −69.2 ± 5.4 mV in 200 μM Cd^{2+}. This indicates that at any given membrane potential, channels were less likely to be inactivated when 200 μM Cd^{2+} was present in the external solution. The slope factors of the availability relationships were unchanged (control = −29.0 ± 1.3 mV, 200 μM Cd^{2+} = −31.4 ± 1.8 mV; $p = 0.2$).

If the observed increases in HERG K^+ current caused by Cd^{2+} result from relief of channel inactivation, then what

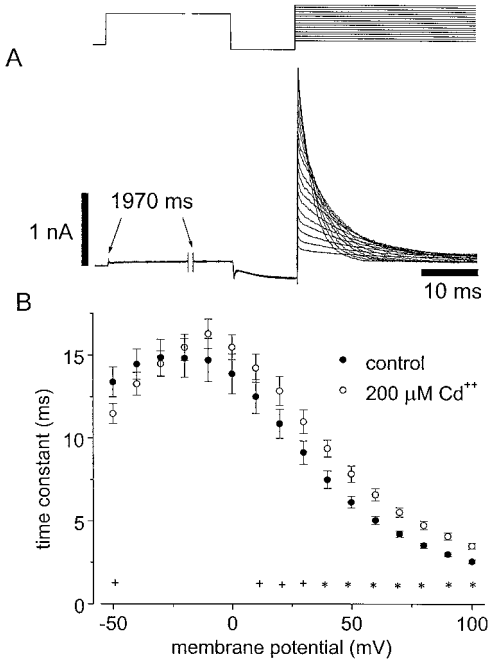

FIGURE 6 Voltage dependence of the rate of inactivation. The voltage clamp protocol at the top of (*A*) was used to measure the voltage dependence. The membrane potential was held at −80 mV before stepping to +60 mV for 2 s to activate the channels. A 12.5-ms step to −100 mV then allows recovery from inactivation before stepping to the test potential between +100 mV and −60 mV. Representative current traces in control conditions are shown at the bottom of (*A*). Note that the time scale bar in (*A*) applies only to the portion of the record after the break. (*B*) A monoexponential equation (see Methods) was used to fit the current inactivation, and the resulting time constants were plotted versus the test membrane potential. The points in (*B*) are averages from eight paired cells with error bars representing the standard error of the mean shown for each point. A paired Student's *t*-test was use to compare differences between means. Significant differences from control are marked along the abscissa (+ = $p < 0.05$; * = $p < 0.001$).

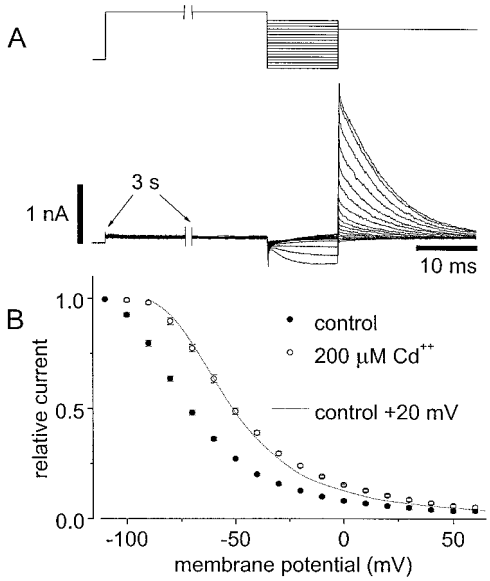

FIGURE 7 Apparent voltage dependence of channel availability. The voltage clamp protocol is shown at the top of (*A*). A typical family of currents in control conditions is shown at the bottom of (*A*). The membrane potential was held at −80 mV before a 3-s step to +90 mV to fully activate the channels. A 12.5-ms test step to potentials between +60 mV and −110 mV was then followed by a step to +30 mV. The peak current observed immediately after stepping to +30 mV was then plotted versus the test potential below in (*B*). Control conditions are indicated by the filled circles. Open circles indicate 200 μM Cd^{2+}. The curves obtained in this way from nine paired cells were normalized to the peak value (−110 mV for control, −100 mV for Cd^{2+}) before averaging. Error bars indicate the standard error of the mean. The dashed line represents the control curve shifted by +20 mV.

happens in channels that do not inactivate? To explore this question, we examined HERG channels containing the double point mutation G628C/S631C. These mutations are in the predicted outer pore of HERG and result in channels with severely impaired inactivation (Smith et al., 1996). Fig. 8, *top left* shows that, unlike wild-type HERG (see Fig. 1), these mutant channels give rise to currents without visible inactivation. Note that in these records the mutant lacked the large tail currents caused by recovery from inactivation in wild-type HERG records. Fig. 8, *top right* and *bottom* show that 200 mM Cd^{2+} did not cause large increases in the mutant channel currents (8 ± 7% increase at +20 mV, $p >$ 0.35; compared to 123 ± 27% in wild-type HERG, see Fig. 3). In addition, Cd^{2+} no longer significantly increased the decay of the tail currents upon repolarization (30 ± 5 ms at −100 mV in control and 21 ± 3 ms in 200 μM Cd^{2+}, $p >$ 0.05) in the G628/S631C mutant channel. These data indicate that the change in the rate of tail current decay seen in wild-type channels most likely did not result from time- and voltage-dependent block of the channel. The ability of Cd^{2+} to increase HERG K^+ current appeared critically dependent upon channel inactivation, and both the increase in current and the accelerated rate of current decay were lost when inactivation was removed. A slight Cd^{2+}-induced increase may be noted in the mutant channel currents (Fig. 8). The most likely explanation for this minor effect is that the mutant channel is not absolutely inactivation-free. This would not be surprising, because many mutations in inactivating K^+ channels can disrupt the inactivation process without completely destroying it (Hoshi et al., 1991; Zou et al., 1998). If the channel retains a small amount of fast inactivation, and the remaining inactivation is still fast relative to channel activation, the current amplitude would be slightly decreased without visible inactivation. Cd^{2+} relief of the residual inactivation would result in a slight current increase.

DISCUSSION

Divalent cations are well known to associate with nonspecific negative charges on the cell surface and change the membrane potential perceived by integral membrane proteins such as K^+ channels (Frankenhaeuser and Hodgkin, 1957; Hammerland et al., 1994; Elinder et al., 1996). Nevertheless, the effects of Cd^{2+} on the rapid delayed rectifying K^+ current of cardiac myocytes (I_{Kr}) cannot be explained by

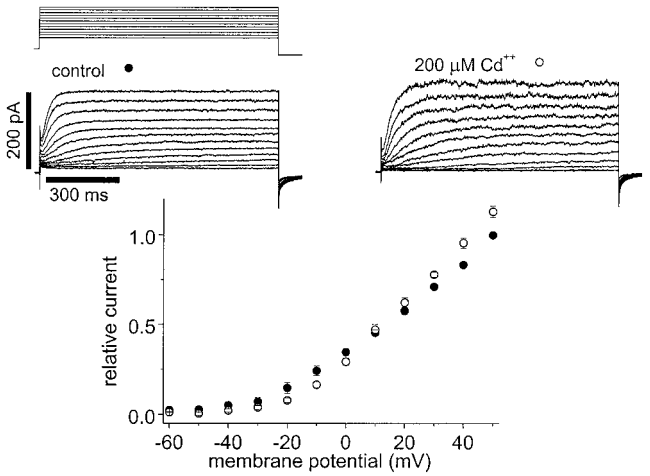

FIGURE 8 A mutant HERG channel with impaired inactivation does not respond normally to Cd^{2+}. Paired current recordings measured from the same cell in control (*top left*) and 200 μM Cd^{2+} (*top right*) solutions. The voltage clamp protocol is shown at the top right. The membrane potential was held at −80 mV before stepping to a test potential between −70 and +50 mV for 1 s. At the end of the test step the potential was stepped to −100 mV. The voltage dependence of channel activation was observed by measuring the current level at the end of the test step and plotting these values versus the test membrane potential (*bottom*). Three cells were tested, each in both conditions. Currents from each cell were normalized to the current level at +50 mV in control solution for that cell. Filled circles indicate control solutions, and open circles indicate 200 μM Cd^{2+}. Error bars indicate the standard error of the mean.

either block or simple shifts alone. In cat and rabbit cardiac myocytes, Cd^{2+} shifts the voltage dependence of activation of I_{Kr} to more depolarized potentials. Nonetheless, Cd^{2+} increased the current evoked at very positive potentials (Follmer et al., 1992; Paquette et al., 1998). A shift in the voltage dependence of activation to more depolarized potentials results in fewer open channels and therefore cannot explain the increase in K^+ current caused by Cd^{2+}. Both Follmer and colleagues (1992) and Paquette et al. (1998) postulated that the increase in I_{Kr} caused by Cd^{2+} might be explained by inhibition of I_{Kr} rectification.

For any K^+ channel, the magnitude of the macroscopic ionic current is determined by the electrochemical driving force for K^+, the number of channels, the single channel conductance, and the open probability of the channel. Open probability is determined by the competing activation and inactivation processes. In HERG channels both processes are voltage-dependent (Wang et al., 1996; Zou et al., 1998; Johnson et al., 1999). Fig. 3 shows that low concentrations of extracellular Cd^{2+} have a unique effect on HERG K^+ currents. Unlike I_{Kr} in cat and rabbit heart, HERG currents show no shift in the voltage dependence of activation until Cd^{2+} concentrations above 200 μM are used, but current is still enhanced. The Cd^{2+}-induced increase is most apparent at positive membrane potentials, where inactivation becomes a primary determinant of channel open probability. This observation can be explained if the equilibrium between the open and inactivated states has been shifted to favor the open state. Therefore, current enhancement is greatest at membrane potentials where inactivation is most prominent. If the mechanism of Cd^{2+} interaction with the channel was generalized charge screening, other divalent cations would have a similar ability to cause this increase in K^+ current (Gilly and Armstrong, 1982). In fact, other divalent cations, such as Ca^{2+} (Ho et al., 1998; Johnson et al., 1999), Mg^{2+} (Po et al., 1999), Ba^{2+} and Zn^{2+} (Ho et al., 1999) decrease, not enhance, HERG currents, further strengthening the idea that the Cd^{2+} effect is unique and specific. In addition to the increase in K^+ currents, we observed that tail current decay upon repolarization was accelerated by 200 μM Cd^{2+} (Fig. 1). This occurs despite the fact that neither the voltage dependence nor the time dependence of activation is affected by 200 μM Cd^{2+} (Figs. 2, 3, and 5). This apparent paradox can be explained using the simple model shown below.

$$\text{Closed} \leftrightharpoons \text{Open} \leftrightharpoons \text{Inactivated}$$

(Scheme 1)

The linear model above requires that inactivated channels must first return to the open state before deactivating to the closed state. Though clearly an oversimplification of real channel behavior, this model captures the essential features required for discussion. How can changes in inactivation affect the apparent rate of deactivation (tail current decay)? Cd^{2+} destabilization of the inactivated state results in fewer inactivated channels. If a larger proportion of the channels is immediately available to deactivate from the open to the closed state (because they need not first return to the open state from the inactivated state, or because they do so more rapidly), the rate of current decay upon repolarization will be increased. This tail current acceleration is analogous to the "tail current cross-over" phenomenon previously seen in other K^+ channels where application of open channel blockers or inactivation peptides cause slowing of tail current decay (Armstrong, 1971; Zagotta et al., 1990). In Scheme 1 the inactivated state corresponds to the blocked state of such a model. For example, an open channel blocker slows the tail current decay kinetics because the channel tends to first unblock to the open state before returning to the closed state. Cd^{2+}-induced relief of HERG inactivation is analogous to reducing block, and thus the tail current decay becomes faster despite the fact that the actual reaction rate constants of the deactivation process remain unchanged.

We have used simple mathematical models that recapitulate the key features of HERG gating to show that altering the rate constants for inactivation can cause increased current and accelerated tail current decay upon repolarization, similar to the actual results of exposing HERG to Cd^{2+}. Two simple models were tested: a three-state model, as represented by Scheme 1 (model data not shown), and a five-state model (Fig. 9) represented in Scheme 2.

$$\text{Closed} \leftrightharpoons \text{Closed} \leftrightharpoons \text{Closed} \leftrightharpoons \text{Open} \leftrightharpoons \text{Inactivated}$$

(Scheme 2)

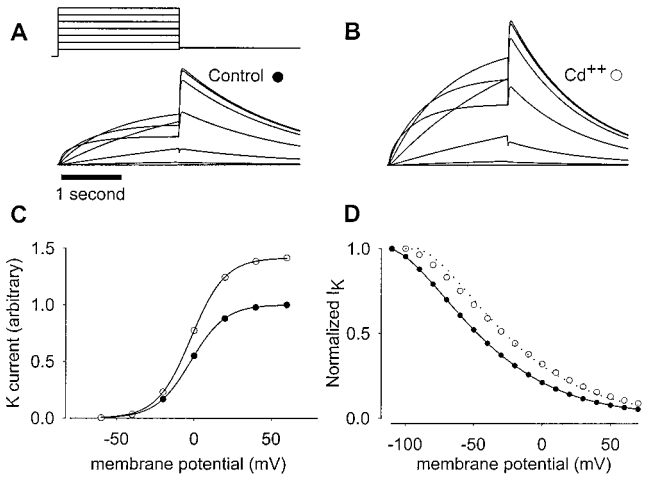

FIGURE 9 Simulation of Cd^{2+} action on HERG potassium channels using the five-state model (C ↔ C ↔ C ↔ O ↔ I) described in Johnson et al. (1999), where C indicates a closed state, O the open state, and I the inactivated state. The model parameters for the simulated control currents were the same as previously described (Johnson et al., 1999). The effect of 200 μM Cd^{2+} was simulated by imposing a +30 mV shift solely on the voltage dependence of the rate constants that govern the transition between open (O) and inactivated (I). The experimental protocols simulated are analogous to data in Figs. 1, 3, and 7. (*A*) Simulated K^+ currents during voltage clamp steps to various membrane potentials (voltage protocol shown in *inset*) followed by step to −50 mV to measure decaying tail currents. (*B*) Same protocol as in (*A*) except the voltage dependence of the inactivation rate constants (O to I) was shifted to simulate the presence of Cd^{2+}. Note the increase in outward K^+ current and the increased rate of tail current decay. (*C*) Tail current amplitude plotted as a function of prepulse potential (compare to Fig. 3, *bottom right*). The filled symbols represent the control condition and the open symbols indicate the voltage-shifted rate constants that occur with 200 μM Cd^{2+}. The maximum current was increased, but no shift in the voltage dependence of these tail currents was observed, similar to the experimental data. (*D*) The pulse protocol was identical to that in Fig. 7. A prepulse to +70 mV was simulated for 3 s followed by a 12.5-ms step to various potentials (compare to Fig. 7) followed by a step to +30 mV. The peak K^+ current during the third step is plotted as a function of potential during the 12.5-ms step. The effect of Cd^{2+} was simulated as in the other panels and is reflected by a +20 mV shift in this relationship, similar to the experimental observation.

The model represented in Fig. 9 was previously published (Johnson et al., 1999) and represents a slight modification of that originally published by Wang et al. (1997a). Fig. 9 shows that a simple shift on the voltage dependence of the rate constants between the open and inactivated states (with no change of the rates between closed states or between closed and open states) reproduces the primary changes seen in upon addition of Cd^{2+} to HERG. Simulated outward currents become larger, the rate of tail current decay is accelerated (Fig. 9, *A* and *B*), and the inactivation availability curve is shifted to more positive potentials (Fig. 9 *D*). The half-maximal voltage of activation in the simulated voltage-dependent activation curve is unaffected, but maximal tail current amplitudes increased (Fig. 9 *C*). Independent of the models, the hypothesis that the increased rate of HERG tail current decay after repolarization is a result of inhibition of inactivation is also supported by the fact that Cd^{2+} does not speed tail current decay upon repolarization in the inactivation-impaired channel (G628C/S631C).

Higher concentrations of Cd^{2+} (0.5–10 mM) shift the voltage dependence of activation (Figs. 4 and 5), but inhibition of inactivation is still present at these levels of extracellular Cd^{2+} because sufficiently strong depolarizations continue to induce currents that are larger than those in control solution (Fig. 4). The shift of the activation voltage dependence by high concentrations of Cd^{2+} could be a result of the divalent cation screening diffuse negative charges on the membrane surface, or could be mediated by a second, lower-affinity, Cd^{2+} site.

HERG K^+ currents are sensitive to the concentration of extracellular K^+. Increasing extracellular K^+ increases outward currents (opposite the prediction of the Nernst equation) and slows channel inactivation (Sanguinetti et al., 1995; Wang et al., 1997b; Yang et al., 1997). This leads to the question of whether Cd^{2+} might interact at the same site as K^+ to facilitate current increase. However, in many respects, the effects of these two ions on HERG currents are quite different. Though elevated extracellular K^+ clearly slows the rate of HERG inactivation, Wang et al. (1997b) showed that the reduction in channel inactivation induced by extracellular K^+ did not account for the current increase seen. Furthermore, elevating K^+ does not accelerate the rate of HERG current tail current decay (Sanguinetti et al., 1995; Wang et al., 1997a, b) in contrast to Cd^{2+}. This implies that the action of K^+ is complex, possibly involving multiple mechanisms. Unlike K^+, all of the effects of low concentrations of Cd^{2+} can be explained by simple inhibition of channel inactivation. The differences in the effects of K^+ and Cd^{2+} make it unlikely that these ions interact with an identical and unique site on the channel.

CONCLUSIONS

We conclude that low concentrations of extracellular Cd^{2+} reduce the probability that HERG K^+ channels reside in inactivated states, thereby leading to more open channels and increased K^+ currents. Higher concentrations of Cd^{2+} cause depolarizing shifts of the voltage dependence of channel activation. The ability to modulate HERG inactivation by an extracellular ligand suggests a novel approach for enhancement of cardiac K^+ currents. It is conceivable that drugs targeting this site could be useful in treating conditions where underexpression or block of this current (e.g., the congenital or acquired long QT syndrome) lead to arrhythmias.

We thank Drs. Louis J. DeFelice and Christoph Fahlke for their insightful discussions and critique of the manuscript. We also thank Michelle Choi for technical assistance. This project was completed in partial fulfillment of the requirements for the Ph.D. degree in Pharmacology at Vanderbilt University School of Medicine (J.P.J.).

This work was supported by National Institutes of Health Grants T32 HL07411, T32 GM07628, HL 51197, and HL 46681.

REFERENCES

Armstrong, C. M. 1971. Interaction of tetraethylammonium ion derivatives with the potassium channels of giant axons. *J. Gen. Physiol.* 58: 413–437.

Choy, A. M., C. C. Lang, D. M. Chomsky, G. H. Rayos, J. R. Wilson, and D. M. Roden. 1997. Normalization of acquired QT prolongation in humans by intravenous potassium. *Circulation.* 96:2149–2154.

Elinder, F., M. Madeja, and P. Århem. 1996. Surface charges of K channels. Effects of strontium on five cloned channels expressed in Xenopus oocytes. *J. Gen. Physiol.* 108:325–332.

Follmer, C. H., N. J. Lodge, C. A. Cullinan, and T. J. Colatsky. 1992. Modulation of the delayed rectifier, IK, by cadmium in cat ventricular myocytes. *Am. J. Physiol.* 262:C75–C83.

Frankenhaeuser, B., and A. L. Hodgkin. 1957. The action of calcium on the electrical properties of squid axons. *J. Physiol. (Lond.).* 137:218–244.

Gilly, W. F., and C. M. Armstrong. 1982. Divalent cations and the activation kinetics of potassium channels in squid giant axons. *J. Gen. Physiol.* 79:965–996.

Hamill, O. P., A. Marty, E. Neher, B. Sakmann, and F. J. Sigworth. 1981. Improved patch-clamp techniques for high-resolution current recording from cells and cell-free membrane patches. *Pflügers Arch.* 391:85–100.

Hammerland, L. G., A. S. Parihar, E. F. Nemeth, and M. C. Sanguinetti. 1994. Voltage-activated potassium currents of rabbit osteoclasts: effects of extracellular calcium. *Am. J. Physiol.* 267:C1103–C1111.

Ho, W. K., Y. E. Earm, and A. W. Lee. 1998. Voltage dependent block of HERG potassium channels by calcium and magnesium. *J. Physiol. (Lond.).* 507.3:631–638.

Ho, W. K., I. Kim, C. 0. Lee, J. B. Youm, S. H. Lee, and Y. E. Earm. 1999. Blockade of HERG channels expressed in *Xenopus laevis* oocytes by external divalent cations. *Biophys J.* 76:1959–1971.

Hoshi, T., W. N. Zagotta, and R. W. Aldrich. 1991. Two types of inactivation in Shaker K+ channels: effects of alterations in the carboxy-terminal region. *Neuron.* 7:547–556.

Johnson, J. P., Jr., F. M. Mullins, and P. B. Bennett. 1999. HERG K^+ channel gating probed with extracellular Ca^{++}: evidence for two distinct voltage sensors. *J. Gen. Physiol.* 113:565–580.

Jurman, M. E., L. M. Boland, Y. Liu, and G. Yellen. 1994. Visual identification of individual transfected cells for electrophysiology using antibody-coated beads. *Biotechniques.* 17:876–881.

Paquette, T., J. R. Clay, A. Ogbaghebriel, and A. Shrier. 1998. Effects of divalent cations on the E-4031-sensitive repolarization current, I(Kr), in rabbit ventricular myocytes. *Biophys. J.* 74:1278–1285.

Po, S. S., D. W. Wang, I. C. H. Wang, J. P. Johnson, Jr., L. Nie, and P. B. Bennett. 1999. Modulation of HERG potassium channels by extracellular magnesium, and quinidine. *J. Cardiovasc. Pharmacol.* 33:181–185.

Rampe, D., M. L. Roy, A. Dennis, and A. M. Brown. 1997. A mechanism for the proarrhythmic effects of cisapride (Propulsid): high affinity blockade of the human cardiac potassium channel HERG. *FEBS Lett.* 417:28–32.

Roy, M., R. Dumaine, and A. M. Brown. 1996. HERG, a primary human ventricular target of the nonsedating antihistamine terfenadine. *Circulation.* 94:817–823.

Sanguinetti, M. C., M. E. Curran, P. S. Spector, and M. T. Keating. 1996. Spectrum of HERG K+-channel dysfunction in an inherited cardiac arrhythmia. *Proc. Natl. Acad. Sci. USA.* 93:2208–2212.

Sanguinetti, M. C., C. Jiang, M. E. Curran, and M. T. Keating. 1995. A mechanistic link between an inherited and an acquired cardiac arrhythmia: HERG encodes the IKr potassium channel. *Cell.* 81: 299–307.

Schönherr, R., and S. H. Heinemann. 1996. Molecular determinants for activation and inactivation of HERG, a human inward rectifier potassium channel. *J. Physiol. (Lond.).* 493:635–642.

Smith, P. L., T. Baukrowitz, and G. Yellen. 1996. The inward rectification mechanism of the HERG cardiac potassium channel. *Nature (Lond.).* 379:833–836.

Spector, P. S., M. E. Curran, A. Zou, M. T. Keating, and M. C. Sanguinetti. 1996. Fast inactivation causes rectification of the IKr channel. *J. Gen. Physiol.* 107:611–619.

Trudeau, M. C., J. W. Warmke, B. Ganetzky, and G. A. Robertson. 1995. HERG, a human inward rectifier in the voltage-gated potassium channel family. *Science (Wash., D.C.).* 269:92–95.

Wang, S., S. Liu, M. J. Morales, H. C. Strauss, and R. L. Rasmusson. 1997a. A quantitative analysis of the activation and inactivation kinetics of HERG expressed in *Xenopus* oocytes. *J. Physiol. (Lond.).* 502:45–60.

Wang, S., M. J. Morales, S. Liu, H. C. Strauss, and R. L. Rasmusson. 1996. Time, voltage and ionic concentration dependence of rectification of h-erg expressed in *Xenopus* oocytes. *FEBS Lett.* 389:167–173.

Wang, S., M. J. Morales, S. Liu, H. C. Strauss, and R. L. Rasmusson. 1997b. Modulation of HERG affinity for E-4031 by [K+]o and C-type inactivation. *FEBS Lett.* 417:43–47.

Warmke, J. W., and B. Ganetzky. 1994. A family of potassium channel genes related to eag in Drosophila and mammals. *Proc. Natl. Acad. Sci. USA.* 91:3438–3442.

Yang, T., D. J. Snyders, and D. M. Roden. 1997. Rapid inactivation determines the rectification and [K+]o dependence of the rapid component of the delayed rectifier K+ current in cardiac cells. *Circ. Res.* 80:782–789.

Zagotta, W. N., T. Hoshi, and R. W. Aldrich. 1990. Restoration of inactivation in mutants of Shaker potassium channels by a peptide derived from ShB. *Science (Wash., D.C.).* 250:568–571.

Zou, A., Q. P. Xu, and M. C. Sanguinetti. 1998. A mutation in the pore region of HERG K+ channels expressed in *Xenopus* oocytes reduces rectification by shifting the voltage dependence of inactivation. *J. Physiol. (Lond.).* 509:129–137.